Quasi-Free-Standing Epitaxial Graphene on SiC Obtained by Hydrogen Intercalation

C. Riedl,[1] C. Coletti,[1] T. Iwasaki,[1] A. A. Zakharov,[2] and U. Starke[1,*]

[1]*Max-Planck-Institut für Festkörperforschung, Heisenbergstr. 1, D-70569 Stuttgart, Germany*

[2]*MAX-Lab, Lund University, Box 118, Lund, S-22100, Sweden*

(Received 8 October 2009; published 10 December 2009)

Quasi-free-standing epitaxial graphene is obtained on SiC(0001) by hydrogen intercalation. The hydrogen moves between the $(6\sqrt{3} \times 6\sqrt{3})$R30° reconstructed initial carbon layer and the SiC substrate. The topmost Si atoms which for epitaxial graphene are covalently bound to this buffer layer, are now saturated by hydrogen bonds. The buffer layer is turned into a quasi-free-standing graphene monolayer with its typical linear π bands. Similarly, epitaxial monolayer graphene turns into a decoupled bilayer. The intercalation is stable in air and can be reversed by annealing to around 900 °C.

DOI: 10.1103/PhysRevLett.103.246804 PACS numbers: 73.20.At, 73.63.−b

Graphene, a monoatomic layer of graphite, displays outstanding electronic, optical, mechanical, and thermal properties which make it extremely appealing for a wide range of applications [1,2]. Grown on hexagonal silicon carbide (SiC) wafers, large area epitaxial graphene samples appear feasible and integration in existing device technology can be envisioned [2–4]. And indeed, the achievement of large-scale homogeneity is on the way [5]. While epitaxial graphene on SiC(000$\bar{1}$) allows only for a poor thickness control and the graphene grows with rotational disorder [2,6,7], on SiC(0001) a defined number of epitaxially ordered graphene layers can be grown [4,5,8]. However, an intrinsic electron doping ($n \approx 10^{13}$ cm^{-2}) is observed [3,4] which originates from the influence of the $(6\sqrt{3} \times 6\sqrt{3})$R30° reconstructed interface layer [8,9] present between graphene and SiC. This interface or buffer layer is constituted of carbon atoms which are arranged in a graphenelike honeycomb structure. However, as depicted in the model sketch in Fig. 1(a), about 30% of these carbon atoms are bound to the Si atoms of the SiC(0001) surface [10,11], which prevents π bands with the linear dispersion typical for graphene to develop in this layer. Thus, the interface layer is electronically inactive in terms of the typical graphene properties so that it is often called zero-layer graphene. The second carbon layer grows on top of the interface without covalent interlayer bonds as shown in Fig. 1(b) and electronically acts like monolayer graphene. The influence of the covalent bonding in the interface layer is also one of the primary suspects for the strongly reduced mobility in epitaxial graphene on SiC(0001) as compared to exfoliated graphene flakes, probably due to the introduction of scattering centers into the graphene layer. So, for a practical application of epitaxial graphene on SiC(0001) it would be desirable to counteract the intrinsic doping and to reduce the influence of the interface bonding to create quasi-free-standing layers.

Reduction of the intrinsic charge carrier density by surface transfer doping has been achieved recently by means of deposited tetrafluoro-tetracyanoquinodimethane (F4-TCNQ) molecules [12] or atomic layers of Bi and Sb [13]. Elimination of the covalent bonding at the interface in order to decouple the epitaxial graphene layers from the SiC substrate would require us to break and saturate the respective bonds. As sketched for zero- and monolayer graphene in Figs. 1(c) and 1(d), we demonstrate in the present Letter that hydrogen intercalation can induce the desired decoupling. As a result the outstanding properties of graphene can be made accessible in quasi-free-standing epitaxial graphene layers on large-scale SiC(0001) wafers suitable for a practical technological application.

For our experiments, on-axis oriented 4H- and 6H-SiC (0001) samples doped with nitrogen (10^{17} to 10^{18} cm^{-3} range) were prepared by chemical-mechanical polishing or hydrogen etching [14,15] in order to get a regular array of atomically flat terraces. The epitaxial graphene layers were prepared by graphitization under ultrahigh vacuum conditions [3,4,8] or in an induction furnace under Ar atmosphere [5]. After transport through air, the samples were annealed at temperatures between 600 °C and 1000 °C in molecular hydrogen at atmospheric pressures. The process was carried out in a chemical vapor deposition reactor in an

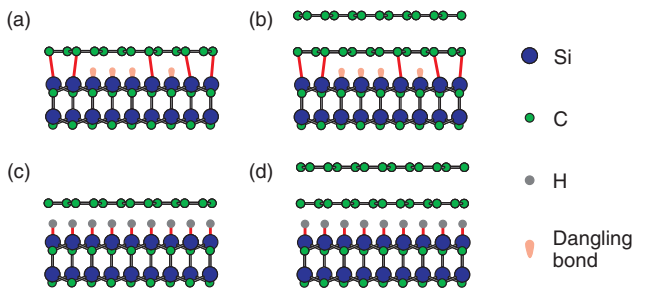

FIG. 1 (color). Side view models for (a) the $(6\sqrt{3} \times 6\sqrt{3})$R30° reconstruction of SiC(0001) (''zero-layer'') and (b) epitaxial monolayer graphene. After hydrogen intercalation (c) the zero-layer and (d) monolayer graphene are decoupled from the substrate.

atmosphere of palladium-purified ultrapure molecular hydrogen, similar to the technique used for hydrogen etching [14,15] and hydrogen passivation [16–18] of SiC surfaces. Angle-resolved photoelectron spectroscopy (ARPES) using monochromatized He II radiation, low energy electron diffraction and microscopy (LEED, LEEM), and core level photoemission spectroscopy (CLPES) were used to analyze the structural, electronic and morphological properties of the epitaxial graphene layers after hydrogen intercalation and the effect of subsequent annealing. The CLPES experiments were carried out using synchrotron radiation at beam line I311 [19] of the MAX radiation laboratory (Lund, Sweden), the LEEM experiments with the LEEMIII instrument at this beam line.

Figures 2(a) and 2(b) display LEED patterns for the $(6\sqrt{3} \times 6\sqrt{3})$R30° reconstructed buffer layer before and after hydrogen treatment. For the pristine buffer layer [panel (a)] the LEED pattern shows intense superstructure spots corresponding to the pronounced atomic displacements in this layer due to the covalent bonding to the SiC substrate [8]. After hydrogen treatment, the superstructure spots are strongly suppressed as depicted in panel (b), which indicates much smaller atomic displacements in the reconstructed layers which in turn suggests the absence or weakening of the interlayer bonding. Similarly, for an epitaxial monolayer the spots of the $(6\sqrt{3} \times 6\sqrt{3})$R30° superstructure vanish upon hydrogen treatment (not shown). This is already a clear indication of a geometrical decoupling of the interface layer from the substrate.

Apart from this structural aspect, the hydrogen treatment has a dramatic effect on the electronic structure of the samples. This is shown in Fig. 3 by ARPES measurements of the valence band structure around the $\bar{K}$ point of the graphene Brillouin zone. For a pristine zero layer no π bands are observed as displayed in panel (a). Only two very faint delocalized and smeared out states at binding energies of around 0.1 eV to 0.5 eV and higher than 0.9 eV are visible. For a zero-layer sample after hydrogen treatment, quite differently, the linear dispersing π bands of monolayer graphene appear, see panel (b). In addition, while as-grown monolayer graphene is n doped, so that its Fermi level E_F is located about 420 meV above the crossing point of the π bands (Dirac point, E_D), as shown below [Fig. 3(f)], this effect is reversed after the hydrogen treatment and the sample is slightly p doped so that E_F is shifted below E_D by ≈100 meV. The appearance of the graphene type π bands and the absence of n doping corroborates our working hypothesis that the covalently bound carbon layer is decoupled from the substrate. Apparently, the hydrogen atoms migrate under this layer, break the bonds between C and Si and bind to the Si atoms as sketched in Figs. 1(a) and 1(c). Correspondingly, the buffer layer is lifted and displays the electronic properties of a quasi-free-standing graphene monolayer. Note, that outgassing the hydrogen treated sample at 400 °C as carried out for the spectrum shown in Fig. 3(b) has no effect on the π band structure. Yet, after heating the sample up to 700 °C [panel (c)] the slight p doping vanishes and charge neutrality is retrieved ($E_F = E_D$), so that we tentatively attribute the p-doping effect to the presence of chemisorbed species on the graphene surface and the subsequent downshift of the band structure to their desorption [20]. At temperatures above 700 °C the π bands progressively weaken as indicated in panel (d). Since Si-H bonds are known to break at temperatures just above 700 °C [21], this effect can be correlated to progressive hydrogen desorption. Around 900 °C the hydrogen has completely desorbed and the zero-layer structure is re-established as seen from the absence of π bands [Fig. 3(e)] and also from the LEED pattern which is similar again to the one shown in Fig. 2(a). Consistent results were observed for monolayer epitaxial graphene, which turns into bilayer graphene upon hydrogen treatment as previously sketched in Figs. 1(b) and 1(d). The corresponding band structure measured by ARPES before hydrogen treatment and after hydrogen treatment plus subsequent outgassing at 400 °C is shown in Figs. 3(f) and 3(g). Again the hydrogen-treated sample shows a slight p doping which disappears after

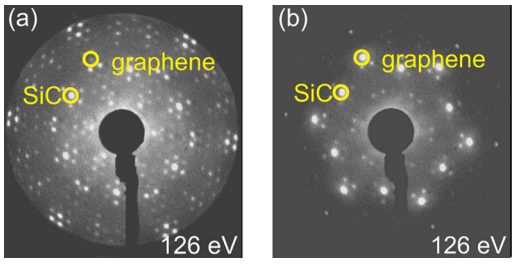

FIG. 2 (color online). LEED patterns at 126 eV for the $(6\sqrt{3} \times 6\sqrt{3})$R30° reconstruction (zero-layer graphene) (a) before and (b) after hydrogen intercalation. The first order diffraction spots are indicated for SiC and graphene.

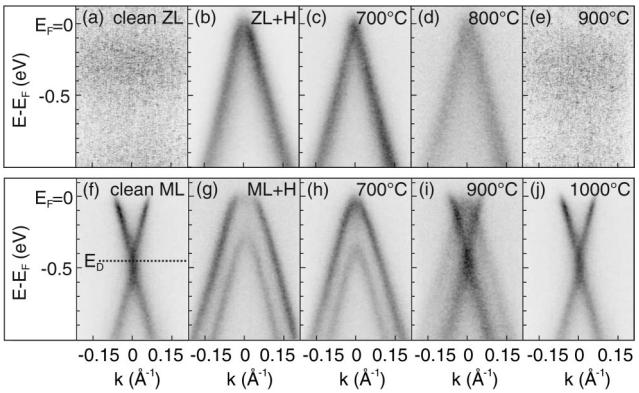

FIG. 3. Dispersion of the π bands measured with ARPES perpendicular to the $\bar{\Gamma}\bar{K}$ direction of the graphene Brillouin zone for (a) an as-grown graphene zero layer (ZL) on SiC(0001), (b) after hydrogen treatment and (c–e) subsequent annealing steps; (f) for an as-grown monolayer (ML), (g) after hydrogen treatment and (h–j) subsequent annealing steps.

annealing to 700 °C [panel (h)]. For temperatures higher than 700 °C the intensity of the bilayer π bands decreases while the monolayer bands reappear [Figs. 3(i) and 3(j)]. The hydrogen progressively desorbs until at 1000 °C the original monolayer band structure is completely recovered.

To corroborate the structural models sketched in Fig. 1, a detailed analysis of the chemical bonds was conducted by using CLPES. Since the resulting picture is very similar for zero-layer and monolayer graphene only the monolayer results will be discussed. Si $2p$ and C $1s$ core level spectra were measured for the hydrogen-treated monolayer sample annealed at different temperatures, as depicted in Fig. 4. Different components contributing to the spectra were decomposed by a curve-fitting procedure [22]. The depth position of the corresponding species within the surface was identified by varying the incident photon energy and thus changing the surface sensitivity; the energies shown in Fig. 4 are 140 eV and 450 eV for the Si $2p$ and C $1s$ spectra, respectively. The experimental data points are displayed in black dots. The gray solid line is the envelope of the fitted components. The bottom curve in Fig. 4(a) shows the C $1s$ spectrum measured after outgassing the hydrogen-treated sample at a temperature around 600 °C. The dominant peak at 284.6 eV is the graphene related component (red line) while the broader, less intense peak at 283.0 eV is the SiC (bulk) related component (dark blue line). We emphasize the complete absence of components related to the $(6\sqrt{3} \times 6\sqrt{3})$R30° reconstruction [10], which clearly identifies the surface as a quasi-free-standing epitaxial graphene layer (bilayer in this case). At annealing temperatures higher than 700 °C the hydrogen starts to desorb, as indicated by the appearance of the interface components S1 and S2, marked with light blue lines. They result from the carbon atoms in the $(6\sqrt{3} \times 6\sqrt{3})$R30° structure [10]. The hydrogen desorption implicates the appearance of a second graphene related peak (black line), representing those patches where the hydrogen has left. For an annealing temperature of 830 °C, this monolayer component becomes more significant than the one resulting from the quasi-free bilayer patches. After annealing at 1000 °C the hydrogen is completely desorbed: the C $1s$ spectrum acquires the shape typically obtained for epitaxial monolayer graphene. The difference in binding energy location between the monolayer and decoupled bilayer components is about 0.4 eV, which perfectly agrees with the shift of the Fermi level measured via ARPES. The total shift of the SiC component is 1 eV, which confirms that on the SiC surface hydrogen bonds are present which cause a respective band bending.

Further evidence of the existence of Si-H bonds is brought by the Si $2p$ data. The Si $2p$ spectrum obtained after initial outgassing [bottom curve in Fig. 4(b)] consists of two spin-orbit split doublets. The binding energies are given with respect to the Si $2p_{3/2}$ component. According to the surface sensitivity variations and in agreement with Ref. [21], the dominant peak at 100.6 eV (dark blue line) can be assigned to the bulk component and the one at 100.9 eV (red line) to Si-H bonds. After annealing at

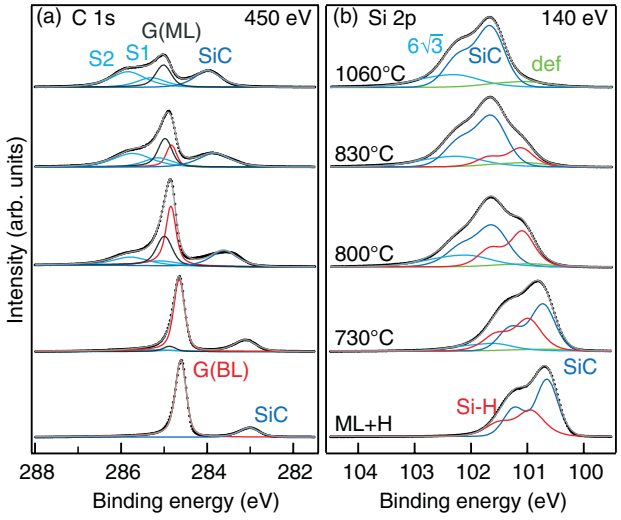

FIG. 4 (color). C $1s$ (a) and Si $2p$ (b) core level spectra for a hydrogen-treated monolayer graphene sample (bottom spectra) and the same sample annealed at increasing temperatures. The experimental data are displayed in black dots. Different components, accordingly labeled in the spectra, are fitted into the C $1s$ and Si $2p$ regions by a line shape analysis. The gray solid line is the envelope of the fitted components.

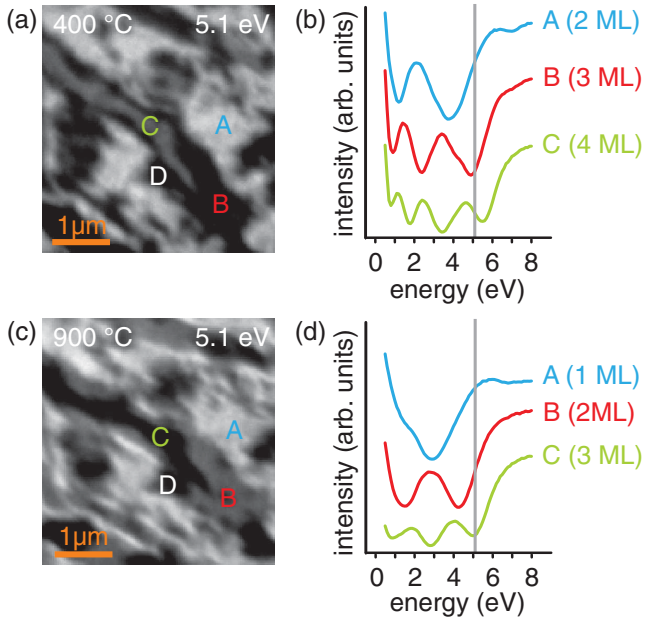

FIG. 5 (color). 4×4 μm^2 LEEM micrographs recorded with an electron energy of 5.1 eV for the same area of (a) a hydrogen-treated graphene sample after outgassing at 400 °C and (c) annealed at 900 °C. Representative regions are labeled A, B, C, D. The electron reflectivity spectra obtained for the regions A, B, and C are plotted in panels (b) and (d), respectively, labeled with the number of graphene monolayers (ML).

730 °C the Si $2p$ spectrum can be accurately fitted only by introducing two additional components: the one at higher binding energy (light blue line) is attributed to the Si atoms bonded to the $(6\sqrt{3} \times 6\sqrt{3})$R30° reconstructed overlayer, the small one at lower binding energy (green line) to surface defects. These components increase in intensity for increasing annealing temperatures while the Si-H component gradually vanishes and completely disappears after annealing at 1000 °C. The total shift observed for the Si $2p$ bulk component amounts to 1 eV in agreement with the C $1s$ bulk peak.

The effect of hydrogen intercalation on the graphene structure can be analyzed with spatial resolution using LEEM, a method that can identify the number of graphene layers on SiC by the number of dips in the electron reflectivity spectra between 0 and 8 eV [23]. In Fig. 5, LEEM micrographs are shown for an electron energy of 5.1 eV measured in the same area of the sample with [panel (a)] and without [panel (c)] intercalated hydrogen. At this energy, regions of different graphene thickness can be distinguished by the reflected intensity. The electron reflectivity spectra for the different surface domains A, B, and C as labeled in panel (a) are plotted in panel (b). The number of dips in the spectra identifies region A, B, and C as bi-, tri-, and four-layer graphene. After desorbing the hydrogen through an annealing step at 900 °C, the spatial distribution of these domains does not change as shown in panel (c). However, their LEEM intensity changes and the reflectivity spectra as plotted in panel (d) identify a complete transformation of $(n + 1)$-layer thick areas into (n)-layer thick areas ($n = 1, 2, 3$). Note that the region labeled D in Fig. 5 displays the same intensity before and after desorption of the hydrogen (and a flat reflectivity spectrum) and is attributed to surface defects, e.g., from residual polishing damage.

The question arises as to how the hydrogen migrates both below the interface layer and even through several graphene layers. Recent experimental reports on hydrogen on graphene did not show any evidence for hydrogen penetration through graphene [24–27]. However, in contrast to these experiments we use molecular hydrogen at atmospheric pressures and our graphene samples were annealed up to 1000 °C which might facilitate a reactive passage of the hydrogen through the graphene lattice. Another possibility is that the hydrogen intercalation starts at grain boundaries or defects on the surface. On a final note, we point out that the hydrogen intercalated samples are extremely stable in ambient atmosphere, at least for several months. Furthermore, hydrogen passivation and desorption can be repeated several times without notable changes in the sample quality.

In summary, we have demonstrated that hydrogen can migrate through epitaxial graphene and the interface layer, bind to the Si atoms of the SiC(0001) surface and decouple epitaxial graphene from its substrate. n-layer graphene films transform into $(n + 1)$-layer graphene films ($n = 0$, 1, 2, 3). The intercalation opens up the possibility to produce quasi-free-standing epitaxial graphene on large SiC wafers. The hydrogen passivates the underlying SiC substrate similar to the case of bare SiC surfaces [16–18]. The intercalated hydrogen is sustained in ambient conditions and stable up to 700 °C. The intercalation process is technologically well adapted and represents a highly promising route towards epitaxial graphene based nanoelectronics.

Support by the EC through the Access to Research Infrastructure Action is gratefully acknowledged. C. C. and T. I. acknowledge the Alexander von Humboldt Foundation for financial support.

*u.starke@fkf.mpg.de; http://www.fkf.mpg.de/ga

[1] A. K. Geim, Science **324**, 1530 (2009).
[2] C. Berger *et al.*, Science **312**, 1191 (2006).
[3] T. Ohta *et al.*, Science **313**, 951 (2006).
[4] C. Riedl, A. A. Zakharov, and U. Starke, Appl. Phys. Lett. **93**, 033106 (2008).
[5] K. V. Emtsev *et al.*, Nature Mater. **8**, 203 (2009).
[6] F. Hiebel *et al.*, Phys. Rev. B **78**, 153412 (2008).
[7] U. Starke and C. Riedl, J. Phys. Condens. Matter **21**, 134016 (2009).
[8] C. Riedl *et al.*, Phys. Rev. B **76**, 245406 (2007).
[9] P. Mallet *et al.*, Phys. Rev. B **76**, 041403 (2007).
[10] K. V. Emtsev *et al.*, Phys. Rev. B **77**, 155303 (2008).
[11] A. Mattausch and O. Pankratov, Phys. Rev. Lett. **99**, 076802 (2007).
[12] C. Coletti, C. Riedl, D. S. Lee, B. Krauss, K. v. Klitzing, J. H. Smet, and U. Starke, arXiv:0909.2966.
[13] I. Gierz *et al.*, Nano Lett. **8**, 4603 (2008).
[14] S. Soubatch *et al.*, Mater. Sci. Forum **483–485**, 761 (2005).
[15] C. L. Frewin *et al.*, Mater. Sci. Forum **615–617**, 589 (2009).
[16] H. Tsuchida, I. Kamata, and K. Izumi, J. Appl. Phys. **85**, 3569 (1999).
[17] T. Seyller, J. Phys. Condens. Matter **16**, S1755 (2004).
[18] C. Coletti, C. L. Frewin, A. M. Hoff, and S. E. Saddow, Electrochem. Solid-State Lett. **11**, H285 (2008).
[19] J. N. Andersen *et al.*, Synchrotron Radiation News **4**, 15 (1991).
[20] D. S. Lee *et al.*, Nano Lett. **8**, 4320 (2008).
[21] N. Sieber *et al.*, Phys. Rev. B **67**, 205304 (2003).
[22] A linear background was subtracted from the Si $2p$ data and a Shirley background from the C $1s$ data. The C $1s$ graphene related peak was fitted using a Doniach-Sunjic profile to account for the metallic behavior, all the other fitted lines are an approximation of the Voigt function.
[23] H. Hibino *et al.*, Phys. Rev. B **77**, 075413 (2008).
[24] D. C. Elias *et al.*, Science **323**, 610 (2009).
[25] A. Bostwick *et al.*, Phys. Rev. Lett. **103**, 056404 (2009).
[26] N. P. Guisinger *et al.*, Nano Lett. **9**, 1462 (2009).
[27] R. Balog *et al.*, J. Am. Chem. Soc. **131**, 8744 (2009).